



## Cytotoxic linear acetylenes from a marine sponge *Pleroma* sp.



Emi Takanashi<sup>a</sup>, Kentaro Takada<sup>a,\*</sup>, Masahiro Hashimoto<sup>b</sup>, Yoshiyuki Itoh<sup>b</sup>, Yuji Ise<sup>c</sup>,  
Susumu Ohtsuka<sup>d</sup>, Shigeru Okada<sup>a</sup>, Shigeki Matsunaga<sup>a,\*</sup>

<sup>a</sup>Laboratory of Aquatic Natural Products Chemistry, Graduate School of Agricultural and Life Sciences, The University of Tokyo, Bunkyo-ku, Tokyo 113-8657, Japan

<sup>b</sup>Japan JEOL Ltd., Akishima, Tokyo 196-8558, Japan

<sup>c</sup>Sugashima Marine Biological Laboratory, Nagoya University, Toba, Mie 517-0004, Japan

<sup>d</sup>Takehara Marine Science Station, Hiroshima University, Takehara, Hiroshima 725-0024, Japan

### ARTICLE INFO

#### Article history:

Received 1 October 2015

Received in revised form 20 October 2015

Accepted 22 October 2015

Available online 24 October 2015

#### Keywords:

Sponge

Cytotoxic

Linear acetylene

Structure elucidation

### ABSTRACT

Bioassay-guided fractionation of the extract of the rare deep-sea marine sponge *Pleroma* sp. afforded seven new linear acetylenes, yakushynols A–F (**1–6**) and neopetroformyne E (**7**). The structures of **1–7** were determined by a combination of the analysis of spectroscopic data and chemical derivatization. Compounds **1–6** are the first examples of the sponge-derived acetylenes of the size of duryne with oxidation at the sixth carbon from the terminus. Compounds **1–5** and **7** exhibited moderate cytotoxic activity. A biosynthetic route of neopetroformyne A was inferred from the structural transition among sponge-derived linear acetylenes.

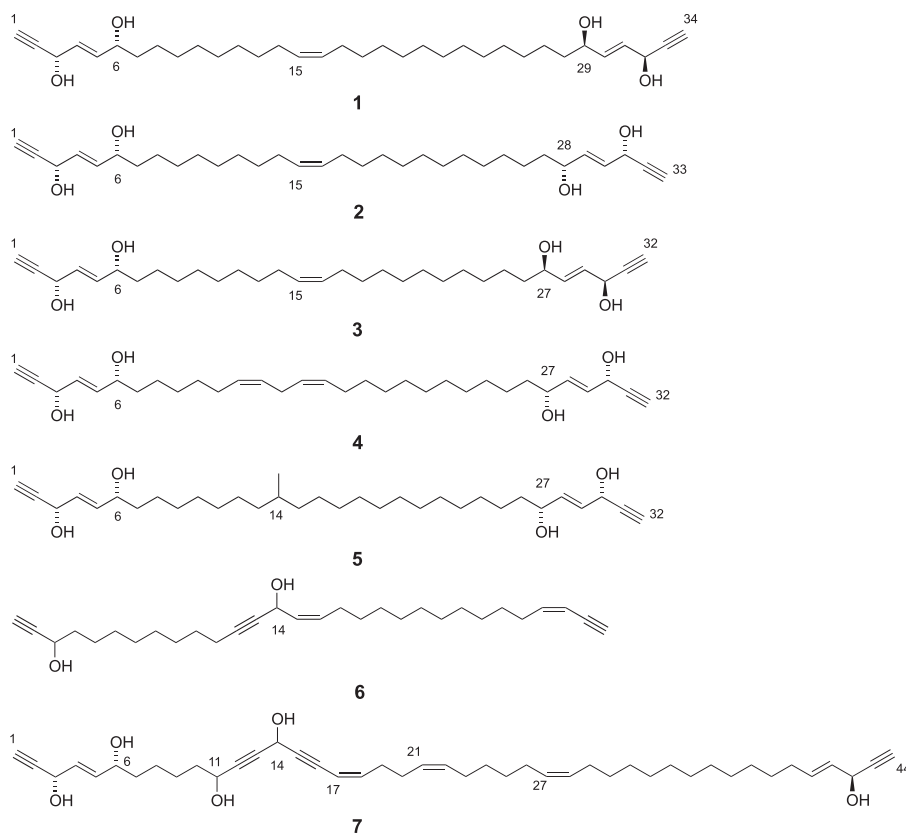
© 2015 Elsevier Ltd. All rights reserved.

## 1. Introduction

Natural products played fundamental roles in drug discovery, particularly in the area of antibiotics and anti cancer agents.<sup>1,2</sup> Because more than 200,000 natural products including more than 30,000 marine natural products have been reported,<sup>3,4</sup> it becomes harder and harder to discover new biologically active natural products, emphasizing the importance of dereplication in natural products discovery study. Natural products are secondary metabolites which, by definition, distribute in living things species

specifically.<sup>5</sup> Therefore, the chance to encounter new secondary metabolites becomes higher, when untapped organisms are studied. This is why we study deep-sea sponges, even though it is not easy to collect the same species of organism again. We use cytotoxic activity to fractionate extracts, because this bioassay is robust and can detect effects against a variety of cellular targets. Historically, many clinical anticancer agents were discovered through this assay.<sup>6</sup> We studied the cytotoxic constituents in the extract of a rare deep-sea marine sponge *Pleroma* sp., which was active in our screening.

\* Corresponding authors. Tel.: +81 3 5841 5297; fax: +81 3 5841 8166; e-mail addresses: [atakada@mail.ecc.u-tokyo.ac.jp](mailto:atakada@mail.ecc.u-tokyo.ac.jp) (K. Takada), [assmats@mail.ecc.u-tokyo.ac.jp](mailto:assmats@mail.ecc.u-tokyo.ac.jp) (S. Matsunaga).



## 2. Results and discussion

The organic extract of the marine sponge *Pleroma* sp. was subjected to solvent partitioning between H<sub>2</sub>O and CHCl<sub>3</sub>, and the CHCl<sub>3</sub> fraction was further partitioned between 90% MeOH and *n*-hexane. The aqueous MeOH fraction, which showed cytotoxic activity, was separated by ODS column chromatography followed by reversed-phase HPLC to afford yakushynols A–F (**1–6**) and neopetroformyne E (**7**).

The molecular formula of yakushynol A (**1**) was established as C<sub>34</sub>H<sub>56</sub>O<sub>4</sub> by HRESIMS. <sup>1</sup>H NMR spectrum showed characteristic signals [ $\delta$  2.90 (H-1 and H-34), 4.82 (H-3 and H-32), 5.73 (H-4 and H-31), and 5.86 (H-5 and H-30)] for the terminal pent-1-en-4-yn-3-ol moiety frequently found in sponge-derived linear acetylenes (C-1 to C-5 and C-30 to C-34),<sup>7</sup> whose presence was confirmed by interpretation of the COSY data. H-5 and H-30 were further coupled to an oxymethine ( $\delta_{\text{H}}$  4.06/ $\delta_{\text{C}}$  72.4), suggesting that the allylic positions (C-6 and C-29) remote from both termini were hydroxylated (Table 1).<sup>8–10</sup> The remaining portion of **1** consisted of a disubstituted double bond and two aliphatic chains. (Fig. 1a). Therefore, this molecule is symmetric or nearly so. The position of the internal double bond was shown to be between C-15 and C-16 on the basis of the high energy-collision induced dissociation (HECID) MS/MS data measured with a MALDI TOF/TOF instrument,<sup>11</sup> in which typical allylic cleavages were observed (Fig. 1b, Fig. S34).<sup>12</sup> The  $\Delta^{15,16}$  assignment was in agreement with the ion peak at *m/z* 257 observed in the negative FABMS of the ozonolysis product with oxidative workup; this ion corresponds to deprotonation product of tetradecanedioic acid, corresponding to the C-16 to C-29 portion in **1**, generated from the initially formed 2-oxopentadecanedioic acid through decarboxylation and oxidation.<sup>13</sup> The geometries of  $\Delta^{4,5}$ - and  $\Delta^{30,31}$ -double bonds were determined as both *E* on the basis of the <sup>1</sup>H–<sup>1</sup>H coupling constant (15.4 Hz), whereas the geometry of  $\Delta^{15,16}$ -double bond was

assigned as *Z* on the basis of the <sup>13</sup>C chemical shift values of 27.9 ppm for the allylic carbons (C-14 and C-17).<sup>14</sup> The absolute configuration of **1** was determined as 3*S*, 6*R*, 29*R*, and 32*S* by the modified Mosher's method (Fig. S2).<sup>15</sup>

**Table 1**  
<sup>1</sup>H and <sup>13</sup>C NMR data for **1** and **4** in CD<sub>3</sub>OD

No	$\delta_{\text{C}}^{\text{a}}$	<b>1</b>	No	$\delta_{\text{C}}^{\text{a}}$	<b>4</b>
		$\delta_{\text{H}}$ ( <i>J</i> in Hz)			
1	74.6	2.90, d (2.1 Hz)	1	74.6	2.90, d (2.1 Hz)
2	84.3		2	84.2	
3	62.5	4.82, brd (5.5)	3	62.5	4.82, brd (5.5)
4	130.3	5.73, ddd (15.4, 5.5, 2.0)	4	130.1	5.73, ddd (15.4, 5.5, 2.0)
5	136.2	5.86, ddd (15.4, 6.4, 1.4)	5	136.1	5.86, ddd (15.4, 6.4, 1.4)
6	72.4	4.06, q (6.4)	6	72.4	4.06, q (6.4)
7	38.1	1.50, m	7	38.1	1.50, m
8	26.3	1.38, m	8	26.3	1.33, m, 1.39, m
9–13	30.5	1.2–1.4	9, 10	30.5	1.2–1.4
14	27.9	2.03, m	11	28.0	2.06, m
15	130.7	5.34, m	12	130.6	5.34, m
16	130.7	5.34, m	13	128.9	5.31, m
17	27.9	2.03, m	14	26.3	2.77, m
18–26	30.5	1.2–1.4	15	128.9	5.31, m
27	26.3	1.38, m	16	130.6	5.34, m
28	38.1	1.50, m	17	28.0	2.06, m
29	72.4	4.06, q (6.4)	18–24	30.5	1.2–1.4
30	136.2	5.86, ddd (15.4, 6.4, 1.4)	25	26.3	1.33, m, 1.39, m
31	130.3	5.73, ddd (15.4, 5.5, 2.0)	26	38.1	1.50, m
32	62.5	4.82, brd (5.5)	27	72.4	4.06, q (6.4)
33	84.3		28	136.1	5.86, ddd (15.4, 6.4, 1.4)
34	74.6	2.90, d ( <i>J</i> =2.1 Hz)	29	130.1	5.73, ddd (15.4, 5.5, 2.0)
			30	62.5	4.82, brd (5.5)
			31	84.2	
			32	74.6	2.90, d ( <i>J</i> =2.1 Hz)

<sup>a</sup> <sup>13</sup>C chemical shifts were determined from the HSQC and HMBC data.

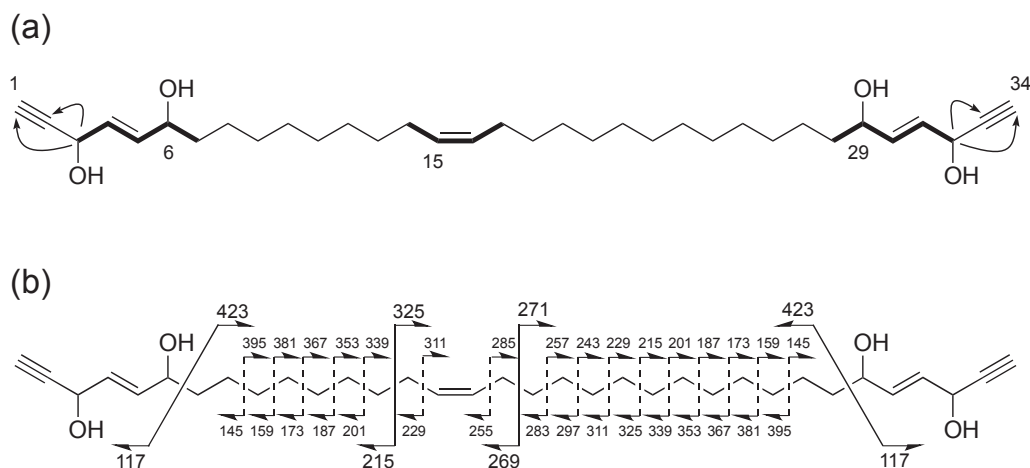


**Fig. 1.** (a) Key COSY and HMBC correlations observed in **1**. Bold lines and arrows show COSY and HMBC correlations, respectively. (b) HE-CID MS/MS data for **1**. Prominent product ion peaks are shown.

Yakushynol B (**2**) and yakushynol C (**3**) had the molecular formula of  $C_{33}H_{54}O_4$  and  $C_{32}H_{52}O_4$ , respectively, as determined by HRESIMS. Their  $^1H$  NMR and HSQC spectra were superimposable on those of **1** except for the integration of the large methylene peak ( $\delta$  1.30), implying that **2** and **3** were lower homologues of **1**. Intense product ions due to allylic cleavages ( $m/z$  215 and 243) in the tandem FAB/MS of **3** revealed that the isolated double bond was located at C-15, which indicated that the longer aliphatic chain in **3** (C-17 to C-26) was shorter than that of **1** by two carbon atoms.<sup>13</sup> We were not able to obtain interpretable MS/MS data of **2** due to the paucity of the sample. The position of the internal double bond in **2** was determined by ozonolysis with oxidative work-up, which gave the  $[M-H]^-$  ion at  $m/z$  229 corresponding to dodecanedioic acid, suggesting that the double bond in **2** was located between C-15 and C-16. The absolute configurations of **2** and **3** were determined by using a simplified version of the modified Mosher's method.<sup>15,16</sup>

The molecular formula of  $C_{32}H_{50}O_4$  as assigned for yakushynol D (**4**) by HRESIMS implied that **4** had one more unsaturation than **3**.

There was a doubly allylic methylene carbon ( $\delta_H$  2.77,  $\delta_C$  26.3). The positions of the two internal double bonds were determined as  $\Delta^{12,13}$  and  $\Delta^{15,16}$  on the basis of the tandem FAB/MS data ( $m/z$  173, 243, 267, and 337), featuring the characteristic ions derived from allylic cleavages.<sup>12</sup> The absolute configuration of **4** was determined by the modified Mosher's method.<sup>15,16</sup>

Yakushynol E (**5**), with the molecular formula of  $C_{33}H_{56}O_4$ , had a branched methyl group in the middle of a saturated linear aliphatic chain. The location of the branched methyl group was assigned as described previously,<sup>17–22</sup> i.e., the intensities of fragment ions for the positional isomers of methyl group were predicted based on the different degree of propensity of cleavage among the C–C bonds around the methyl branch and compared with the observed spectrum. The incidence of the cleavage of the C–C bonds between the methyl-substituted methine carbon and the adjacent methylene carbons was approximately twice as frequent as those between the neighboring C–C bonds remote from the branching point (Fig. 2).<sup>17</sup> The observed product ion spectrum

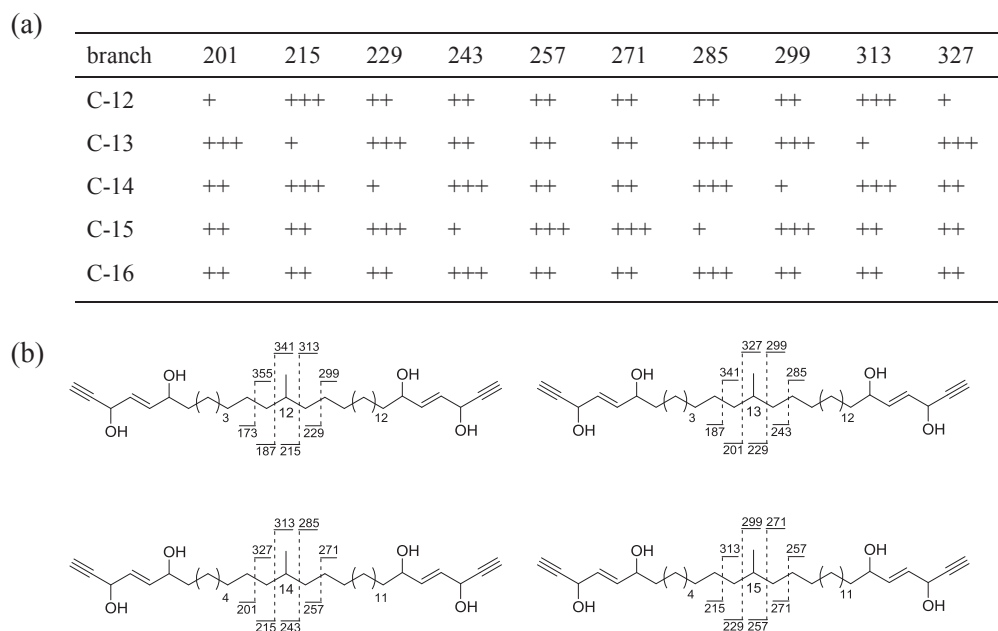


**Fig. 2.** Prediction of the intensities of product ions for the molecules with the branched methyl group at C-12, C-13, C-14, C-15, or C-16. (a) The expected intensity of each ion peak was represented by the number of +. (b) Expected fragmentation pattern of the molecules with methylation at C-12, C-13, C-14, and C-15.

with significant decreased intensities of the ions at  $m/z$  229 and 299 matched well with that of the predicted spectrum when the methyl group was located at C-14 (Fig. 2 and S37).<sup>18–22</sup> The absolute configuration of **5** was determined as 3*S*, 6*R*, 27*R*, and 30*S* by the modified Mosher's method (Fig. S2). The configuration at C-14 was not determined.

The molecular formula of yakushynol F (**6**) was C<sub>30</sub>H<sub>46</sub>O<sub>4</sub> as determined by HRESIMS. NMR data implied that **6** was a congener of corticatynol A (Table 2).<sup>23</sup> Compound **6** had an additional oxygenated methine at C-14, and the  $\Delta^{4,5}$ -olefin in corticatynol A was saturated in **6**. The lengths of the two methylene chains were determined by HE-CID MS/MS.<sup>12</sup> The *Z*-geometry of  $\Delta^{15,16}$ -double bond was assigned on the basis of the <sup>13</sup>C chemical shift of C-17 (27.8 ppm), whereas the *Z*-geometry of the  $\Delta^{27,28}$ -double bond was assigned by a <sup>1</sup>H–<sup>1</sup>H coupling constant of 10.8 Hz between H-27 and H-28. Due to the paucity of the sample, the absolute configuration of **6** was not determined.

**Table 2**  
<sup>1</sup>H and <sup>13</sup>C NMR data for **6** and **7** in CD<sub>3</sub>OD

No	$\delta_C^a$	<b>6</b>	No	$\delta_C^a$	<b>7</b>
		$\delta_H$ (J in Hz)			$\delta_H$ (J in Hz)
1	72.5	2.77, d (2.1 Hz)	1	75.0	2.90, d (2.1 Hz)
2	85.0		2	84.8	
3	62.4	4.26, dt (2.1, 6.5)	3	62.7	4.82, brd (5.8)
4	38.7	1.64, m	4	130.5	5.75, ddd (15.5, 6.2, 1.0)
5	26	1.2–1.4	5	136.3	5.87, ddd (15.5, 6., 1.42)
6–9	30.0	1.2–1.4	6	72.4	4.08, q (6.5)
10	29.1	1.48, m	7	38.2	1.53, m
11	19.1	2.20, dt (2.0, 6.7)	8	26	1.38, m
12	84.4		9	26	1.30, m
13	81.4		10	38.5	1.49, m, 1.67, m
14	58.5	5.05, qd (2.0, 5.2)	11	62.5	4.35, dt (1.7, 6.7)
15	132.0	5.45, m	12	85.9	
16	131.5	5.45, m	13	83.1	
17	27.8	2.02, m	14	52.8	5.27, t (1.9)
18–24	30	1.2–1.4	15	92.4	
25	29.3	1.41, m	16	81.1	
26	30.8	2.30, q (7.2)	17	109.5	5.50, dq (1.7, 10.6)
27	146.2	6.00, dt (10.8, 7.2)	18	145.4	5.99, dt (10.7, 7.3)
28	109.1	5.45, m	19	31.4	2.37 dq (1.3, 7.5)
29	<sup>b</sup>		20	27.5	2.17, q (7.2)
30	81.7	3.41, d (J=2.1 Hz)	21	129.7	5.38, m
			22	131.7	5.36, m
			23	28	2.05, m
			24–25	30	1.2–1.4
			26	28.0	2.05, m
			27	130.9	5.36, m
			28	130.9	5.36, m
			29	28.0	2.05, m
			30–38	30	1.2–1.4
			39	32.6	2.04, m
			40	134.2	5.85, ddd (15.5, 6.9, 1.1)
			41	130.5	5.55, ddt (15.2, 6.5, 1.4)
			42	62.7	4.73, brd (6.2)
			43	84.8	
			44	74.8	2.87, d (J=2.1 Hz)

<sup>a</sup> <sup>13</sup>C chemical shifts were assigned from the HSQC and HMBC data.

<sup>b</sup> Not assigned.

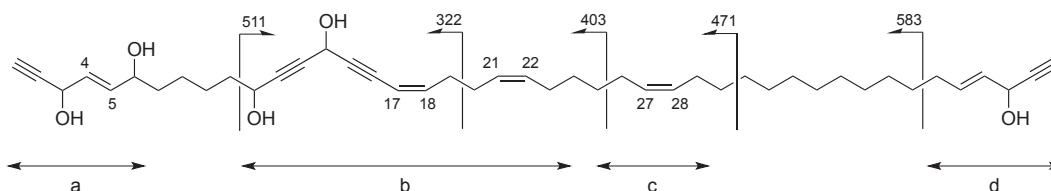


**Fig. 3.** The HE-CID MS/MS data for **7** using the  $[M+Li]^+$  ion as the precursor. Partial structures described in the text are shown by arrows.

Neopetroformyne E (**7**) had a molecular formula of C<sub>44</sub>H<sub>64</sub>O<sub>5</sub> as determined by HRESIMS. <sup>1</sup>H NMR and HSQC spectra of **7** were reminiscent of those of neopetroformynes (Table 2).<sup>24</sup> Interpretation of the 2D NMR data disclosed four partial structures (Fig. 3). Partial structure **a** (C-1 to C-6) was identical with the terminal portion of **1**. A structural unit similar to partial structure **b** (C-11 to C-23) was found in neopetroformyne A.<sup>24</sup> However the geometry of the conjugated double bond was reversed. Partial structure **c** (C-26 to C-29) was an isolated disubstituted double bond and partial structure **d** (C-39 to C-44) was the conventional pent-1-en-4-yn-3-ol unit.<sup>12</sup> The locations and orientation of partial structure **b** and **c** were assigned by interpretation of the MALDI HE-CID MS data in which diagnostic fragment ion peaks were observed at  $m/z$  322,<sup>25</sup> 403, 511, and 583 (Fig. 3 and S34).<sup>13</sup> The geometries of  $\Delta^{4,5}$ - and  $\Delta^{40,41}$ -double bonds were assigned as both *E* on the basis of the <sup>1</sup>H–<sup>1</sup>H coupling constants. The geometries of  $\Delta^{17,18}$ -,  $\Delta^{21,22}$ -, and  $\Delta^{27,28}$ -double bonds were assigned as all *Z* on the basis of the <sup>13</sup>C chemical shifts of the allylic methylene carbons. 3*S*, 6*R*, and 42*S* configuration was assigned for **7** by the modified Mosher's method. However, configurations of C-11 and C-14 were not determined due to the ambiguous results in the modified Mosher's analysis.

Compounds **1–5** and **7** exhibited cytotoxic activity against HeLa cells with IC<sub>50</sub> values of 5.2, 10.8, 1.1, 12.2, 4.8, and 2.5  $\mu$ g/mL, respectively. Compound **6** did not show cytotoxicity at a dose of 50  $\mu$ g/mL.

In our previous report on the structure elucidation of corticatic acid A,<sup>23</sup> we proposed a biosynthetic pathway of duryne, in which we pointed out that the positionally conserved central double could be the vestige of condensation of two fatty acids (Fig. 4a). In **1–4**, the position of the central double bond was also conserved. The relationship of the positions of the methylation in **5** and the unsaturation in **3** is also observed between miyakosyne A and duryne.<sup>12,18</sup> The biogenesis of the carbinol-interrupted diyne moiety as found in neopetroformynes has been enigmatic.<sup>7,26</sup> We predicted the propensity of the biochemical transformation within the sponge by comparing the structures of congeners. The presence of **3** and **4** suggests that the shorter alkyl chain of **3** is subjected to desaturation, whereas the structure of **6** indicates that the newly formed double bond in **4** is further desaturated and the methylene carbon flanked by a double bond and a triple bond is oxidized. We have noticed that if such series of desaturation and allylic oxidation events occurred at around C-14 in the recently reported isofulvinol,<sup>27–29</sup> this compound would be converted into neopetroformyne A (Fig. 4b).

### 3. Experimental section

#### 3.1. General procedures

Optical rotations were measured on a JASCO DIP-1000 digital polarimeter. NMR spectra were recorded on a JEOL JNM-ECA600 NMR spectrometer at 600 MHz for <sup>1</sup>H and 150 MHz for <sup>13</sup>C. <sup>1</sup>H and <sup>13</sup>C chemical shifts were referenced to the solvent peaks at  $\delta_H$  3.30 and  $\delta_C$  49.0 for CD<sub>3</sub>OD. Electrospray ionization (ESI) mass spectra were measured on a JEOL JMS-T100LC 'AccuTOF' liquid

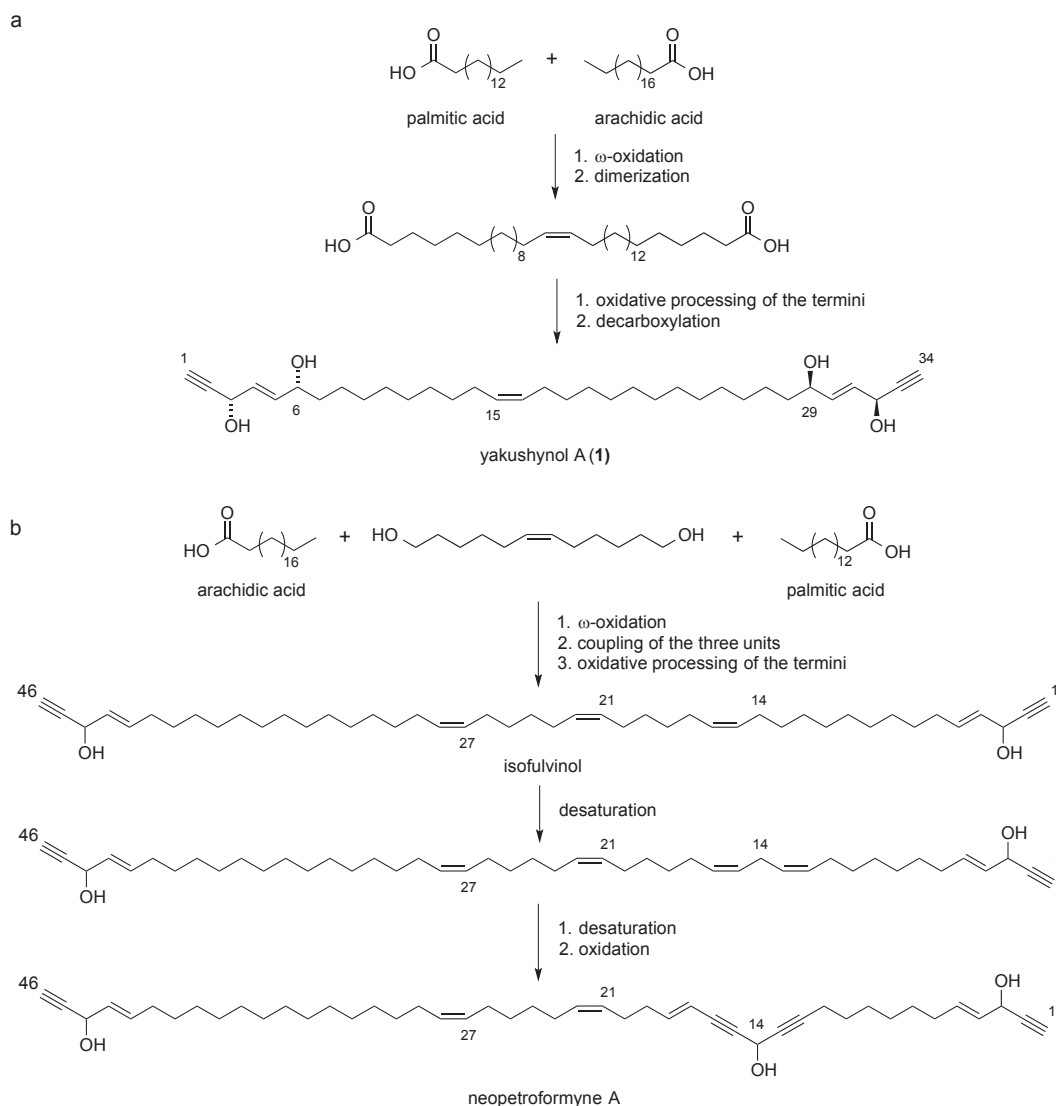


Fig. 4. A possible biosynthetic pathway of (a) yakushynol A (1) and (b) neopetroformyne A.

chromatograph—time-of-flight (TOF) mass spectrometer (MS). Fast atom bombardment (FAB) mass spectra and FAB—high-energy collision-induced dissociation (HE-CID) product ion mass spectra were measured on a JEOL JMS-700T 'MStation' 4-sector tandem MS. Matrix-assisted laser desorption/ionization (MALDI) mass spectra and MALDI HE-CID product ion mass spectra were measured on a JEOL JMS-S3000 'Spiral TOF' MALDI-TOF-TOF tandem MS.

### 3.2. Animal material

The sponge *Pleroma* sp. was collected by dredging at a depth of ca. 200 m at the seamount 'Yaku-Shin Sone' (29°49.29'N, 130°24.56'E), south off Yakushima Island, southern Japan, during the cruise of R/V Toyoshio-maru, 18 May 2011. Sponge description: dented cup shaped with hispid surface due to protruding long oxeas; consistency stony hard; the color in life beige. Ectosomal skeleton made of dichotriaenes and long oxeas traversing choanosome and protruding from surface of the sponge. Choanosomal skeleton consisted of dense articulation of megaclone desmas. Microscleres abundant acanthomicroxeas, microrhabds, streptasters/metasters, and rare tiny spirasters. Dichotriaene having straight rhabd with blunt tip; size of the rhabd 958 (825–1075)

$\mu\text{m}$  in length, 40.2 (35.0–47.5)  $\mu\text{m}$  in width, the radius of the cladome 354 (275–438)  $\mu\text{m}$ . Long oxea very thin, straight or slightly arched, sharply pointed at both extremities, measuring 1.4 (1.3–1.8) mm in length, 7.8 (5.0–12.5)  $\mu\text{m}$  in width. Megaclone desma smooth with monaxial crepis of 77 (70–85)  $\mu\text{m}$  in length. Thick epirhabd bearing three to four clones radiate in one direction forming tripods or quadripods. Epirhabd 136 (115–165)  $\mu\text{m}$  in width. The zygomes spherical and cup-shaped, 185 (150–230)  $\mu\text{m}$  in diameter. Acanthomicroxeas almost uniform in shape and size, fusiform, slightly arched at midpoint of the spicule, sharply pointed at both extremities, with uniformly rough surface, measuring 153 (150–165)  $\mu\text{m}$  in length, 3.2 (2.5–4.0)  $\mu\text{m}$  in width. Microrhabds irregular shape, subspherical, oval, sinuous to zigzag, with microspined rough surface, measuring 11.1 (8.8–13.8)  $\mu\text{m}$  in length, 4.7 (3.8–5.0)  $\mu\text{m}$  in width. Streptasters/metasters bearing more than eight long actines, measuring 15.8 (12.5–20.0)  $\mu\text{m}$  in length (including spine length). Spirasters very rare and tiny, bearing small spines on convex side of its shaft, measuring 7.5  $\mu\text{m}$  in length and less than 1.5  $\mu\text{m}$  in width. The spicule component of the present material is very similar to *Pleroma menoui* Lévi & Lévi,<sup>30</sup> according to Kelly.<sup>31</sup> However sizes of the spicules are different between the two specimens: dichotriaene,

acanthomicroxea, and microrhabds are much larger in *P. menoui*, and crepis of the megaclone is longer in the present specimen. Furthermore, geographical distribution of the both species is distant: *P. menoui* has been reported only from deep sea of the southern hemisphere such as Lord Howe and Norfolk Islands, New Caledonia and New Zealand.<sup>30,31</sup> Hence here we tentatively regard our specimen as different species from *P. menoui*. The specimen used for the identification (NSMT-Po-2482) is deposited at National Museum of Nature and Science, Tokyo.

### 3.3. Extraction and isolation

The sponge specimen was frozen after collection and kept frozen until extraction. The sample (1 kg) was extracted with MeOH (2×3 L) and CHCl<sub>3</sub>/MeOH (1:1) (1×3 L). The extracts were combined, evaporated, and partitioned between H<sub>2</sub>O and CHCl<sub>3</sub> (3×500 mL). The CHCl<sub>3</sub> fraction was further partitioned between 90% MeOH and *n*-hexane. The aqueous MeOH fraction was separated by ODS flash chromatography with aq MeOH and CHCl<sub>3</sub>–MeOH (1:1) to afford six fractions. An active fraction was separated by reversed-phase HPLC (Cosmosil MS-II, 20×250 mm) with 70–100% MeOH to afford yakushynol B (**2**, 1.6 mg), C (**3**, 8.7 mg), and D (**4**, 4.8 mg). Another active fraction was purified by reversed-phase HPLC (COSMOSIL AR-II, 10×250 mm) with 80% MeOH to give yakushynol A (**1**, 1.6 mg), E (**5**, 1.4 mg), neopetroformyne E (**7**, 0.4 mg), and yakushynol F (**6**, 0.6 mg).

### 3.4. Yakushynol A (1)

Pale yellow oil;  $[\alpha]_D^{21} +11$  (c 0.07, MeOH); UV (MeOH)  $\lambda_{\max}$  (log  $\epsilon$ ) 205 (3.60); <sup>1</sup>H NMR (CD<sub>3</sub>OD, 600 MHz) and <sup>13</sup>C NMR (CD<sub>3</sub>OD, 150 MHz) data, see Table 1; HRESIMS *m/z* 551.4119 [M+Na]<sup>+</sup> (calcd for C<sub>34</sub>H<sub>56</sub>O<sub>4</sub>Na, 551.4076).

### 3.5. Yakushynol B (2)

Pale yellow oil;  $[\alpha]_D^{22} +55$  (c 0.08, MeOH); UV (MeOH)  $\lambda_{\max}$  (log  $\epsilon$ ) 208 (3.68); <sup>1</sup>H NMR (CD<sub>3</sub>OD, 600 MHz): 5.86 (H-5, H-29), 5.73 (H-4, H-30), 5.34 (H-15, H-16), 4.81 (H-3, H-31), 4.06 (H-6, H-28), 2.89 (H-1, H-33), 2.03 (H-14, H-17), 1.50 (H-7, H-27), 1.2–1.4 (H-8 to H-13, H-18 to H-26); <sup>13</sup>C NMR (CD<sub>3</sub>OD, 150 MHz): 136.2 (C-5, C-29), 130.7 (C-15, C-16), 130.3 (C-4, C-30), 84.3 (C-2, C-32), 74.6 (C-1, C-33), 72.4 (C-6, C-28), 62.5 (C-3, C-31), 38.1 (C-7, C-27), 30.5 (C-9 to C-13, C-18 to C-25), 27.9 (C-14, C-17), 26.3 (C-8, C-26); HRESIMS *m/z* 537.3893 [M+Na]<sup>+</sup> (calcd for C<sub>33</sub>H<sub>54</sub>O<sub>4</sub>Na, 537.3920).

### 3.6. Yakushynol C (3)

Pale yellow oil;  $[\alpha]_D^{22} -65$  (c 0.23, MeOH); UV (MeOH)  $\lambda_{\max}$  (log  $\epsilon$ ) 206 (3.67); <sup>1</sup>H NMR (CD<sub>3</sub>OD, 600 MHz): 5.86 (H-5, H-28), 5.73 (H-4, H-29), 5.34 (H-15, H-16), 4.81 (H-3, H-30), 4.06 (H-6, H-27), 2.89 (H-1, H-32), 2.03 (H-14, H-17), 1.50 (H-7, H-26), 1.2–1.4 (H-8 to H-13, H-18 to H-25); <sup>13</sup>C NMR (CD<sub>3</sub>OD, 150 MHz) 136.2 (C-5, C-28), 130.7 (C-15, C-16), 130.3 (C-4, C-29), 84.3 (C-2, C-31), 74.6 (C-1, C-32), 72.4 (C-6, C-27), 62.5 (C-3, C-30), 38.1 (C-7, C-26), 30.5 (C-9 to C-13, C-18 to C-24), 27.9 (C-14, C-17), 26.3 (C-8, C-25); HRESIMS *m/z* 523.3737 [M+Na]<sup>+</sup> (calcd for C<sub>32</sub>H<sub>52</sub>O<sub>4</sub>Na, 523.3763).

### 3.7. Yakushynol D (4)

Pale yellow oil;  $[\alpha]_D^{22} -49$  (c 0.15, MeOH); UV (MeOH)  $\lambda_{\max}$  (log  $\epsilon$ ) 263 (3.39), 215 (3.74); <sup>1</sup>H NMR (CD<sub>3</sub>OD, 600 MHz) and <sup>13</sup>C NMR (CD<sub>3</sub>OD, 150 MHz) data, see Table 1; HRESIMS *m/z* 521.3616 [M+Na]<sup>+</sup> (calcd for C<sub>32</sub>H<sub>50</sub>O<sub>4</sub>Na, 521.3607).

### 3.8. Yakushynol E (5)

Pale yellow oil;  $[\alpha]_D^{19} +41$  (c 0.06, MeOH); UV (MeOH)  $\lambda_{\max}$  (log  $\epsilon$ ) 194 (3.45); (CD<sub>3</sub>OD, 600 MHz): 5.86 (H-5, H-29), 5.73 (H-4, H-30), 4.81 (H-3, H-31), 4.06 (H-6, H-28), 2.89 (H-1, H-33), 1.50 (H-7, H-27), 1.37 (H-14), 1.2–1.4 (H-8 to H-12, H-16 to H-26), 1.29 (H-13 and H-15), 1.08 (H-13 and H-15), 0.85 (14-Me); <sup>13</sup>C NMR (CD<sub>3</sub>OD, 150 MHz): 136.2 (C-5, C-28), 130.3 (C-4, C-29), 84.3 (C-2, C-31), 74.6 (C-1, C-32), 72.4 (C-6, C-27), 62.5 (C-3, C-30), 38.1 (C-7, C-26), 37.9 (C-13, C-15), 33.6 (C-14), 30.5 (C-8 to C-11, C-17 to C-26), 27.0 (C-12, C-16), 26.3 (C-8, C-25), 20.0 (14-Me); HRESIMS *m/z* 539.4054 [M+Na]<sup>+</sup> (calcd for C<sub>33</sub>H<sub>56</sub>O<sub>4</sub>Na, 539.4076).

### 3.9. Yakushynol F (6)

Pale yellow oil;  $[\alpha]_D^{22} +43$  (c 0.03, MeOH); UV (MeOH)  $\lambda_{\max}$  (log  $\epsilon$ ) 222 (3.39), 215 (3.38), 204 (3.49); <sup>1</sup>H NMR (CD<sub>3</sub>OD, 600 MHz) and <sup>13</sup>C NMR (CD<sub>3</sub>OD) data, see Table 2; HRESIMS *m/z* 461.3348 [M+Na]<sup>+</sup> (calcd for C<sub>30</sub>H<sub>46</sub>O<sub>2</sub>Na, 461.3396).

### 3.10. Neopetroformyne E (7)

Pale yellow oil;  $[\alpha]_D^{21} +150$  (c 0.02, MeOH); UV (MeOH)  $\lambda_{\max}$  (log  $\epsilon$ ) 229 (3.85), 206 (3.73); (CD<sub>3</sub>OD, 600 MHz) and <sup>13</sup>C NMR (CD<sub>3</sub>OD, 150 MHz) data, see Table 2; HRESIMS *m/z* 695.4645 [M+Na]<sup>+</sup> (calcd for C<sub>44</sub>H<sub>64</sub>O<sub>5</sub>Na, 695.4651).

### 3.11. Preparation of MTPA esters

To a solution of the compound (**1**: 0.1 mg, **3**: 80  $\mu$ g, **4**: 0.1 mg, **5**: 0.1 mg, **7**: 50  $\mu$ g) in dry pyridine (10  $\mu$ L) was added (*R*)-MTPACl (2  $\mu$ L). The solutions were left at room temperature for 24 h, and the reaction mixtures were diluted with H<sub>2</sub>O and extracted with CHCl<sub>3</sub>. The organic layers were purified by reversed-phase HPLC to afford the (*S*)-MTPA esters. (*R*)-MTPA esters of compound **1**, **2**, and **5** were prepared in a similar way using (*S*)-MTPACl.

### 3.12. Tetra-(*S*)-MTPA ester of 1 (1a)

(CD<sub>3</sub>OD, 600 MHz)  $\delta$  7.45, 7.39, 7.38, 6.09 (H-3, H-32), 5.88 (H-5, H-30), 5.69 (H-4, H-31), 5.45 (H-6, H-29), 5.33 (H-15, H-16), 3.50 (OMe), 2.65 (H-1, H-34), 2.02 (H-14, H-17), 1.68 (H-7, H-28), 1.62 (H-7, H-28), 1.2–1.4; ESIMS *m/z* 1415 [M+Na]<sup>+</sup>.

### 3.13. Tetra-(*R*)-MTPA ester of 1 (1b)

<sup>1</sup>H NMR (CD<sub>3</sub>OD, 600 MHz)  $\delta$  7.48, 7.40, 7.40, 6.13 (H-3, H-32), 6.11 (H-5, H-30), 5.95 (H-4, H-31), 5.52 (H-6, H-29), 5.34 (H-15, H-16), 3.48 (OMe), 2.65 (H-1, H-34), 2.02 (H-14, H-17), 1.63 (H-7, H-28), 1.61 (H-7, H-28), 1.2–1.4; ESIMS *m/z* 1415 [M+Na]<sup>+</sup>.

### 3.14. Tetra-(*R*)-MTPA ester of 2 (2b)

(CD<sub>3</sub>OD, 600 MHz)  $\delta$  7.45, 7.39, 7.38, 6.09 (H-3, H-31), 5.88 (H-5, H-29), 5.69 (H-4, H-30), 5.45 (H-6, H-28), 5.33 (H-15, H-16), 3.50 (OMe), 2.65 (H-1, H-33), 2.02 (H-14, H-17), 1.68 (H-7, H-27), 1.62 (H-7, H-27), 1.2–1.4; ESIMS *m/z* 1401 [M+Na]<sup>+</sup>.

### 3.15. Tetra-(*S*)-MTPA ester of 3 (3a)

(CD<sub>3</sub>OD, 600 MHz)  $\delta$  7.45, 7.39, 7.38, 6.09 (H-3, H-30), 5.88 (H-5, H-28), 5.69 (H-4, H-29), 5.45 (H-6, H-27), 5.33 (H-15, H-16), 3.50 (OMe), 2.65 (H-1, H-32), 2.02 (H-14, H-17), 1.68 (H-7, H-26), 1.62 (H-7, H-26), 1.2–1.4; ESIMS *m/z* 1387 [M+Na]<sup>+</sup>.

### 3.16. Tetra-(S)-MTPA ester of 4 (4a)

(CD<sub>3</sub>OD, 600 MHz)  $\delta$  7.45, 7.39, 7.38, 6.09 (H-3, H-30), 5.88 (H-5, H-28), 5.69 (H-4, H-29), 5.45 (H-6, H-27), 5.33, 5.20, 3.50 (OMe), 2.75 (H-14), 2.65 (H-1, H-32), 2.02 (H-11, H-17), 1.68 (H-7, H-26), 1.62 (H-7, H-26), 1.2–1.4; ESIMS  $m/z$  1385 [M+Na]<sup>+</sup>.

### 3.17. Tetra-(S)-MTPA ester of 5 (5a)

(CD<sub>3</sub>OD, 600 MHz)  $\delta$  7.45, 7.39, 7.38, 6.11 (H-3, H-30), 6.11 (H-5, H-28), 5.95 (H-4, H-29), 5.52 (H-6, H-27), 3.50 (OMe), 2.65 (H-1, H-32), 1.63 (H-7, H-28), 1.61 (H-7, H-28), 1.37 (H-14), 1.2–1.4, 0.84 (14-Me); ESIMS  $m/z$  1403 [M+Na]<sup>+</sup>.

### 3.18. Tetra-(R)-MTPA ester of 5 (5b)

(CD<sub>3</sub>OD, 600 MHz)  $\delta$  7.45, 7.39, 7.38, 6.09 (H-3, H-30), 5.88 (H-5, H-28), 5.69 (H-4, H-29), 5.45 (H-6, H-27), 3.50 (OMe), 2.65 (H-1, H-32), 1.68 (H-7, H-27), 1.62 (H-7, H-27), 1.37 (H-14), 1.2–1.4, 0.84 (14-Me); ESIMS  $m/z$  1403 [M+Na]<sup>+</sup>.

### 3.19. Penta-(S)-MTPA ester of 7 (7a)

(CD<sub>3</sub>OD, 600 MHz)  $\delta$  7.45, 7.39, 7.38, 6.50 (H-14), 6.09 (H-3), 6.02 (H-42), 6.00 (H-40), 5.83 (H-5), 5.68 (H-4), 5.51 (H-41), 5.48 (H-6), 3.50 (OMe), 2.65 (H-1, H-44), 2.31, 2.20, 2.11, 1.72 (H-7), 1.2–1.4; ESIMS  $m/z$  1775 [M+Na]<sup>+</sup>.

### 3.20. Ozonolysis

An acetylene (**1–4**, **6**, and **7**) in MeOH was treated with O<sub>3</sub> at –78 °C for 15 min. After the removal of excess O<sub>3</sub> by aeration with O<sub>2</sub>, the solution was dried under a stream of N<sub>2</sub>. The reaction mixture was treated with 90% HCOOH and 30% H<sub>2</sub>O<sub>2</sub> (2:1, 1 mL) and kept at rt for 15 min. The product was concentrated and subjected to FABMS without further purification.

### 3.21. MTT cytotoxicity assay against HeLa cells

Cytotoxicity against HeLa cells was evaluated by MTT assay. Wild type HeLa cells were cultured in Dulbecco's modified Eagle's medium containing 10% fetal bovine serum, 2  $\mu$ g/mL gentamycin, and 2  $\mu$ g/mL antibiotic-antimycotic (Gibco) at 37 °C under an atmosphere of 5% CO<sub>2</sub>. Cell suspension (200  $\mu$ L, 1  $\times$  10<sup>4</sup> cells/mL) in 96-well microplate was incubated for 24 h, followed by addition of each test sample dissolved in DMSO and further incubation for 72 h. Then, 3-(4,5-dimethylthiazol-2-yl)-2,5-diphenyltetrazolium bromide (MTT) saline solution (1 mg/mL, 50  $\mu$ L) was added and incubated for 3 h. After the medium was removed by aspiration, the formazan was extracted with DMSO (150  $\mu$ L). The cell growth inhibition was calculated on the basis of the absorbance at 540 nm. In this assay, adriamycin was used as the positive control for a cytotoxic agent.

### Acknowledgements

This work was partly supported by a Grant-in-Aid for Scientific Research on Innovative Areas 'Chemical Biology of Natural Products'<sup>32</sup> and JSPS KAKENHI Grant Numbers 25252037, 25712024,

25660163, and 15K14799 from The Ministry of Education, Culture, Sports, Science and Technology, Japan.

### Supplementary data

Supplementary data (<sup>1</sup>H NMR and 2D NMR for **1–7**, HE-CID MS for **1**, **5**, **6**, **7**, and tandem FABMS for **3** and **4**) associated with this article can be found in the online version, at <http://dx.doi.org/10.1016/j.tet.2015.10.062>.

### References and notes

- Newman, D. J.; Cragg, G. M.; Snader, K. M. *Nat. Prod. Rep.* **2000**, *17*, 215–234.
- Newman, D. J.; Cragg, G. M. *J. Nat. Prod.* **2012**, *75*, 311–335.
- Dictionary of Natural Product; <http://dnpc.chemnetbase.com/intro> accessed September 30, 2015.
- Dictionary of Marine Natural Products*; Blunt, J. W., Munro, M. H. G., Eds.; Chapman & Hall/CRC: Boca Raton, FL, 2008.
- Torssell, K. B. G. *Natural Products Chemistry*; Swedish Pharmaceutical Press: Stockholm, Sweden, 1997.
- Anticancer Agents from Natural Products*; Cragg, G. M., Kingston, D. G. I., Newman, D. J., Eds.; Taylor & Francis: Boca Raton, FL, 2005.
- Minto, R. E.; Blacklock, B. J. *Prog. Lipid Res.* **2008**, *47*, 233–306.
- Shin, J. H.; Seo, Y. W.; Cho, K. W.; Rho, J. R.; Paul, V. J. *Tetrahedron* **1998**, *54*, 8711–8720.
- Chill, L.; Miroz, A.; Kashman, Y. *J. Nat. Prod.* **2000**, *63*, 523–526.
- Cimino, G.; De Giulio, A.; De Rosa, S.; Di Marzo, V. *J. Nat. Prod.* **1990**, *53*, 345–353.
- Kubo, A.; Satoh, T.; Itoh, Y.; Hashimoto, M.; Tamura, J.; Cody, R. B. *J. Am. Soc. Mass Spectrom.* **2013**, *24*, 684–689.
- Hitora, Y.; Takada, K.; Okada, S.; Ise, Y.; Matsunaga, S. *J. Nat. Prod.* **2011**, *74*, 1262–1267.
- All acetylenes except **5** were subjected to ozonolysis followed by oxidative work-up. The products were subjected to negative mode FABMS. In **1–4**, the prominent ions ( $m/z$  257, 243, 229, and 229, respectively) corresponded to dicarboxylic acids formed by decarboxylation followed by oxidation were observed. Ion peaks were observed at  $m/z$  229 and 243 in the oxidation products of **6** and **7**, respectively.
- Breitmaier, E.; Voelter, W. *Carbon-13 NMR Spectroscopy*; VCH Verlagsgesellschaft: Weinheim, Germany, 1987; pp 192–194; The C-4 carbons of (*E*)- and (*Z*)-2-octene resonate at 33.0 and 27.1 ppm, respectively.
- Ohtani, I.; Kusumi, T.; Kashman, Y.; Kakisawa, H. *J. Am. Chem. Soc.* **1991**, *113*, 4092–4096.
- Due to the scarcity of the samples only one isomer of the MTPA ester was prepared. Because the <sup>1</sup>H NMR chemical shifts of the (*R*)- and (*S*)-MTPA esters were highly conserved in the terminal portions, it was possible to deduce the absolute configuration from the <sup>1</sup>H NMR data of one isomer of MTPA ester.
- Gross, M. L. *Int. J. Mass Spectrom.* **2000**, *200*, 611–624.
- Hitora, Y.; Takada, K.; Okada, S.; Matsunaga, S. *Tetrahedron* **2011**, *67*, 4530–4534. The validity of the methodology used in this paper was confirmed by the following studies.<sup>19–22</sup>
- Inokuma, Y.; Yoshioka, S.; Ariyoshi, J.; Arai, T.; Hitora, Y.; Takada, K.; Matsunaga, S.; Rissanen, K.; Fujita, M. *Nature* **2013**, *495*, 461–466.
- Inokuma, Y.; Yoshioka, S.; Ariyoshi, J.; Arai, T.; Hitora, Y.; Takada, K.; Matsunaga, S.; Rissanen, K.; Fujita, M. *Nature* **2013**, *501*, 262–262.
- Hitora, Y.; Takada, K.; Matsunaga, S. *Tetrahedron* **2013**, *69*, 11070–11073.
- Mori, K.; Akasaka, K.; Matsunaga, S. *Tetrahedron* **2014**, *70*, 392–401.
- Takada, K.; Okada, S.; Matsunaga, S. *Fish. Sci.* **2014**, *80*, 1057–1064.
- Ueoka, R.; Ise, Y.; Matsunaga, S. *Tetrahedron* **2009**, *65*, 5204–5208.
- Okamoto, C.; Nakao, Y.; Fujita, T.; Iwashita, T.; van Soest, R. W. M.; Fusetani, N.; Matsunaga, S. *J. Nat. Prod.* **2007**, *70*, 1816–1819. The fragmentation pathway to generate the even-numbered product ion in the carbinol skipped diynes is discussed in this reference.
- Zhou, Z.-F.; Menna, M.; Cai, Y.-S.; Guo, Y.-W. *Chem. Rev.* **2015**, *115*, 1543–1596.
- Ciavatta, M. L.; Nuzzo, G.; Takada, K.; Mathieu, V.; Kiss, R.; Villani, G.; Gavagnin, M. *J. Nat. Prod.* **2014**, *77*, 1678–1684. For  $\omega$ -oxidation in biological systems, see references 26 and 27.
- Van Bogaart, I. N. A.; Groeneboer, S.; Saerens, K.; Soetaert, W. *FEBS J.* **2011**, *278*, 206–221.
- Miura, Y. *Proc. Jpn. Acad., Ser. B* **2013**, *89*, 370–382.
- Lévi, C.; Lévi, P. *Bull. Mus. Natn. Hist. Nat. 4e ser A* **1983**, *5*, 101–168.
- Kelly, M. N. *Z. J. Mar. Freshwater Res.* **2003**, *37*, 113–127.
- Ueda, M. *Chem. Lett.* **2012**, *41*, 658–666.